A novel technique for unsteady Newtonian fluid flow over a permeable plate with viscous dissipation, non-uniform heat source/sink and chemical reaction

[1]L. Wahidunnisa, [1]K.Subbarayudu, [2*]S. Suneetha

[1]Research Scholar, [2]Assistant Professor, Department of Applied Mathematics, Yogi Vemana University, Kadapa-516005, Andhra Pradesh, INDIA.*suneethayvu@gmail.com

ABSTRACT - This work concentrates on the study of the unsteady Hydromagnetic heat and mass transfer of a Newtonian fluid in a permeable stretching plate with viscous dissipation and chemical reaction. Thermal radiation, velocity slip, concentrate slip are also considered. The unsteady in the flow, temperature and concentration distribution is past by the time dependence of stretching velocity surface temperature and surface concentration. Appropriate similarity transformations are used to convert the governing partial differential equations into a system of coupled non-linear differential equations. The resulting coupled non-linear differential equations are solved numerically by using the fourth order Runge-Kutta method with shooting technique. The impact of various pertinent parameters on velocity, temperature, concentration, skin friction coefficient and the Nusselt number are presented graphically and in tabular form. Our computations disclose that fluid temperature has inverse relationship with the radiation parameter. Comparison between the previously published results and the present numerical results for various for various special cases been done and are found to be an excellent agreement.

Key-words*: *Aligned magnetic field, chemical reaction, viscous dissipation, Thermal radiation, slip effects, heat source /sink.

I. INTRODUCTION

The study of boundary layer flow of heat and mass transfer of stretching surfaces has gained the interest of many researchers because of its extensive applications in many industrial manufacturing processes which include both metal and polymer sheets. Some examples are in the extraction of polymer and rubber sheets, wire drawing, hot rolling, spinning of fibers, metal spinning, paper production, glass blowing, crystal growing, nuclear reactors, cooling of metallic sheets or electronic chips, manufacture of foods, etc., Crane [1] computed an exact similarity solution for the boundary layer flow of a Newtonian fluid toward an elastic sheet which is stretched with the velocity proportional to the distance from the origin. Mohanty et al., [2] developed a model to investigate the heat and mass transfer effect of a micropolar fluid over a stretching sheet through porous media. Mastroberardino [3] found accurate solutions for viscoelastic boundary layer flow and heat transfer over a stretching sheet.

In addition, heat and mass transfer with chemical reaction has special significance in chemical and hydrometallurgical industries. The formation of smog represents a first-order homogeneous chemical reaction. For instance, one can take into account the emission of NO_2 from automobiles and other smoke-stacks. Thus, NO_2 reacts chemically in the atmosphere with unburned hydrocarbons (aided by sunlight) and produces peroxyacetyl nitrate, which forms a layer of photochemical smog. Chemical reactions can be treated as either homogeneous or heterogeneous processes. It depends on whether they occur at an interface or as a single-phase volume reaction. Most of the Chemical reactions involve either heterogeneous or homogeneous processes. Some reactions are very slow or not at all, except in the presence of a catalyst. A complex interaction lies between the homogeneous and heterogeneous reactions which is incorporated in the production and consumption of reactant species at different rates on the fluid and also on the catalytic surfaces, such happen in fog formation and dispersion, food processing, manufacturing of polymer production, groves of fruit trees, moisture over agricultural fields, equipment design by chemical processing, crops damage via freezing etc. Some kind of chemical reaction is observed if there is a foreign mass in air or water. During a chemical reaction, heat is generated between two species (Byron Bird R.et al. [4]). Generally, the reaction rate depends on the concentration of the mass itself. If the rate of reaction is directly proportional to concentration itself (Cussler [5]), then it is said to be first order.

Chemical reactions are classified into two categories; via homogeneous reaction, which involves only single phase reaction and heterogeneous reaction, which involves two or more phases and occur at the interface between the fluid and solid or between two fluids separated by an interface. The important applications of homogeneous reactions are the combination of common household gas and oxygen to produce a flame and the reactions between aqueous solutions of acids and bases. Themelis [6] stated that the

 DOI : 10.18231/2454-9150.2018.1286

majority of chemical reactions encountered in applications are first-order and heterogeneous reactions such as hydrolysis of methyl acetate in the presence of mineral acids and inversion of cane sugar in the presence of mineral acids. A chemical reaction is said to be first-order when a reaction rate depends on a single substance and the value of the exponent is one. Midya [7] observed from their study that the first-order chemical reaction is very important in chemical engineering where the chemical reactions take place between a foreign mass and the working fluid.

MHD problems occur in several situations like the prediction of space weather, damping of turbulent fluctuations in semiconductor melts in crystal growth, measurement of flow rates of beverages in the food industry. It also has applications in geophysics; it is applied to study the stellar and solar structures, interstellar matter, radio propagation through the ionosphere etc. in engineering in MHD pumps, MHD bearings etc. Hayata et al., [8] studied MHD flow of nanofluids over an exponentially stretching sheet in a porous medium with convective boundary conditions. Bala Anki Reddy et al., [9] examined the Numerical Study of MHD Boundary Layer Slip Flow of a Maxwell Nanofluid over an exponentially stretching surface with convective boundary condition. Yan Zhang et al., [10] analyzed the Heat and Mass Transfer in a Thin Liquid Film over an Unsteady Stretching Surface in the Presence of Thermo solutal Capillarity and Variable Magnetic Field.
At high temperatures attained in some engineering devices, gas, for example, can be ionized and so becomes an electrical conductor. The ionized gas or plasma can be made to interact with the magnetic and alter heat transfer and friction characteristic. Since some fluids can also emit and absorb thermal radiation, it is of interest to study the effect of magnetic field on the temperature distribution and heat transfer when the fluid is not only an electrical conductor but also it is capable of emitting and absorbing thermal radiation. This is of interest because heat transfer by thermal radiation has become of greater importance when we are concerned with space applications and higher operating temperatures. Manjula et al., [11] focussed on the influence of Thermal Radiation and Chemical Reaction on MHD Flow. Narayana and Babu [12] studied numerically the MHD heat and mass transfer of a Jeffrey fluid over a stretching sheet with chemical reaction and thermal radiation.

Problems on fluid flow and mass transfer through porous media are the interest of not only mathematicians but also chemical engineers who have generally concerned with reacting and absorbing species, petroleum engineers, who have concerned with the miscible displacement process and civil engineers who are confronted with the problem of salt water encroachment of careful costal equiforce. Also, porous media are very widely used for heated body to maintain its temperature. To make the heat insulation of the surface more effective it is necessary to study the free convective effects underflow through porous media and to estimate effects on the heat transfer. Nayak et al., [13] studied Heat and mass transfer effects on MHD viscoelastic fluid over a stretching sheet through porous medium in presence of chemical reaction. Effect of thermal radiation on unsteady mixed convection flow and heat transfer over a porous stretching surface in porous medium was investigated by Mukhopadhyay[14].

The effect of heat source/sink on heat transfer is another significant aspect in view of many physical problems. Heat generation or absorption may change the heat distribution in the fluid which consequently affects the particle deposition rate in the system such as semiconductors, electronic devices and nuclear reactors. Heat source/sink may be considered constant, space dependent or temperature dependent. Here, we will discuss non-uniform, i.e., space and temperature dependent heat source/sink. Several studies on the heat source/sink and thermal radiation effects and some other related problems were performed by some investigators. [15-18]

In all the revisions declared above, viscous dissipation is neglected. But the viscous dissipation in the natural convective flow is important, when the flow field of extreme size or in high gravitational field. Such effects are important in geophysical flows and also in certain industrial geophysical flows operations and are usually characterized by the Eckert number. Gebhart [19] revealed that a significant viscous dissipation may occur in natural convection in various devices which are subject to large decelerations or which operate at high rotational speeds. Viscous dissipation effects may also be present in stronger gravitational fields and in procedures wherein the scale of the process is very large, e.g., on larger planets, in large grassroots of gas in space, and in geological processes in fluids internal to various bodies. During the movement of fluid particles, viscosity of the fluid converts some kinetic energy into thermal energy. As this process is irreversible and caused due to viscosity, so this is called viscous dissipation. Initially the effect of viscous dissipation was considered by Brickman [20]. Chand et al., [21] studied the effects of viscous dissipation and radiation on unsteady flow of electrically conducting fluid through a permeable stretching surface. Suneetha et al., [22] analyzed the radiation and Mass Transfer Effects on MHD Free Convective Dissipative Fluid in the Presence of Heat Source/Sink. Bala Anki Reddy et al., [23] studied the impact of Cattaneo-Christov heat flux in the Casson fluid flow over a stretching surface with aligned magnetic field and homogeneous heterogeneous chemical reaction.

Generally, a viscous fluid normally sticks to a boundary, i.e., there is no-slip of the fluid relative to the boundary. The no slip boundary state, which is the supposition that a liquid stick to a solid boundary, is one of the pillar of the Navier–Stokes theory. The non-adherence of the fluid to a solid boundary is called velocity slip. Velocity slip may arise on a stretching boundary when the fluid contains particulates such as emulsions, suspensions, foams and polymer solutions. Fluids exhibiting boundary slip also feature in diverse areas such as polishing of artificial heart valves and hydrophobic walls in fuel cells. Simulation of these effects requires modifications to wall boundary conditions which are achieved via the Navier slip model for velocity and a thermal jump slip model for temperature. Additionally, mass (solutal) slip can occur when simultaneous species diffusion occurs. Numerous studies have revealed the important influence of slip on

 DOI : 10.18231/2454-9150.2018.1286

near-wall flow characteristics. Daba et al. [24] studied the unsteady hydromagnetic chemically reacting mixed convection flow over a permeable stretching surface with slip and thermal radiation. Das [25] investigated the convective heat transfer performance of nanofluids from a permeable stretching surface with partial slip, thermal buoyancy and temperature dependent internal heat generation/absorption. Swati [26] shed light on the Slip effects on MHD boundary layer flow over an exponentially stretching sheet with suction/blowing and thermal radiation. Bala Anki Reddy and Suneetha [27] analysed the Effects Of Homogeneous-Heterogeneous Chemical Reaction And Slip Velocity On Mhd Stagnation Flow Of A Micropolar Fluid Over A Permeable Stretching/Shrinking Surface Embedded In A Porous Medium. More recently, several sleuths ([28]-[30]) studied on different fluids.

The intent of the current model is to study the effect of chemical reaction, as well as heat and mass transfer on the MHD fluid flow over an inclined permeable stretching surface with an acute angle α to the vertical in the presence of a non-uniform heat source/sink. Thermal radiation, viscous dissipation, velocity slip, thermal slip and solutal slip conditions are taken into account. The governing partial differential equations have been transformed into a system of ordinary differential equations by similarity transformations which are then solved numerically by using fourth order Runge–Kutta scheme together with the shooting method. The effects of various pertinent parameters on the momentum, heat and mass transfer characteristics have been studied and numerical results are presented graphically and in the tabular form. This paper has been arranged as follows: Section 2 deals with the mathematical formulation of the problem. Section 3 contains numerical results and discussions. The concluding remarks are presented in Sec. 4.

II. MATHEMATICAL FORMULATION

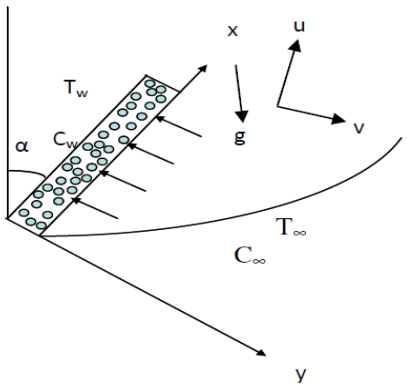

Figure1. Physical sketch of the problem.

Let us consider an unsteady two-dimensional viscous, incompressible, electrically conducting of Newtonian fluid over a permeable time-dependent stretching sheet. The coordinate system and flow model are shown in Fig. 1. At time t=0, the sheet is impulsively stretched with velocity $U_w(x,t)=\frac{ax}{(1-ct)}$ along the x-axis, where the origin is kept fixed in the fluid medium of ambient temperature T_∞.

A magnetic field B(t) is applied perpendicular to the sheet. It is assumed that the magnetic Reynolds number is much less than unity so that the induced magnetic field is negligible in comparison to the applied magnetic field. The velocity slip, thermal slip, solutal slip and first-order homogeneous time-dependent chemical reaction have been taken into account. The fluid properties are assumed to be constant. Under these assumptions, the governing boundary layer equations that are based on the balance laws of mass, linear momentum, energy and concentration species for the blood flow in the presence of thermal radiation take the following form:

$$\frac{\partial u}{\partial x}+\frac{\partial v}{\partial y}=0 \tag{1}$$

$$\frac{\partial u}{\partial t}+u\frac{\partial u}{\partial x}+v\frac{\partial u}{\partial y}=\upsilon\frac{\partial^2 u}{\partial y^2}+g\beta\left(T-T_\infty\right)\cos\alpha + g\beta^*\left(C-C_\infty\right)\cos\alpha-\frac{\sigma B^2(t)}{\rho}Sin^2(\xi)\,u-\frac{\upsilon}{k_1(t)}u \tag{2}$$

$$\frac{\partial T}{\partial t}+u\frac{\partial T}{\partial x}+v\frac{\partial T}{\partial y}=\frac{k}{\rho C_p}\frac{\partial^2 T}{\partial y^2}-\frac{1}{\rho C_p}\frac{\partial q_r}{\partial y} + \frac{q'''}{\rho C_p}+\frac{\upsilon}{C_p}\left(\frac{\partial u}{\partial y}\right)^2 \tag{3}$$

$$\frac{\partial C}{\partial t}+u\frac{\partial C}{\partial x}+v\frac{\partial C}{\partial y}=D\frac{\partial^2 C}{\partial y^2}-\Gamma(t)\left(C-C_\infty\right) \tag{4}$$

Subject to the boundary conditions:

$$u=U_w+N\mu\frac{\partial u}{\partial y}, v=V_w, T=T_w+K\frac{\partial T}{\partial y},$$
$$C=C_w+P\frac{\partial c}{\partial y}\ at\ \ y=0$$
$$u\to 0, T\to T_\infty, C\to C_\infty\ \ as\ y\to\infty \tag{5}$$

where V_w represents the injection/suction velocity given by

$$V_w=-\sqrt{\frac{\upsilon U_w}{x}}\,f(0) \tag{6}$$

Equation (6) implies that the mass transfer at the surface of the capillary wall takes place with a velocity V_w where $V_w>0$ in the case of injection and $V_w<0$ in the case of suction. In Eq. (2), $k_1(t)=k_2(1-ct)$ represents the time-dependent permeability parameter, in Eq. (5), $N=N_0(1-ct)^{\frac{1}{2}}$ is the velocity slip factor. $K=K_0(1-ct)^{\frac{1}{2}}$ is the thermal slip factor and $P=P_0(1-ct)^{\frac{1}{2}}$ is the concentration slip factor. The no-slip conditions can be recovered, by putting

 DOI : 10.18231/2454-9150.2018.1286

N = K = P = 0. The velocity $U_w(x,t)$ of the stretching motion of the blood vessel, surface temperature $T_w(x,t)$ and the concentration $C_w(x,t)$ are considered as

$$U_w = \frac{ax}{1-ct}, T_w = T_\infty + \frac{bx}{1-ct}, C_w = C_\infty + \frac{dx}{1-ct} \quad (7)$$

where a, b, c and *d* are the constants such that $a > 0$, $b \geq 0$, $c \geq 0$, $d \geq 0$ *and* $ct < 1$. Let us consider

$B(t) = B_0(1-ct)^{-\frac{1}{2}}$ *and* $\Gamma(t) = \Gamma_0(1-ct)^{-1}$, where B_0 is a constant representing the magnetic field strength at t =o, Γ_0 is a constant, *u* and *v* are the velocity components in the *x* and *y* directions respectively, ρ is the density of the fluid, g is the acceleration due to gravity, β is the coefficient of thermal expansion, β^* is the coefficient of expansion with concentration, T is the temperature, T_∞ is the temperature of the ambient fluid, *C* is the concentration, C_∞ is the concentration of the ambient fluid, σ is the electrical conductivity, ν is the kinematic viscosity, C_p is the specific heat at constant pressure, *k* is the thermal conductivity, q_r is the radiative heat flux *n*, ξ is the aligned angle and *D* is the mass diffusion coefficient.

The non-uniform heat source/sink, q''' is modeled as

$$q''' = \frac{KU_w(x,t)}{x\nu}\left[A^*(T_w - T_\infty)f' + B^*(T - T_\infty)\right],$$

where A^* and B^* are the coefficient of space and temperature dependent heat source/sink, respectively. It is to be noted that the case $A^* > 0$, $B^* > 0$ corresponds to internal heat generation and that $A^* < 0$, $B^* < 0$ corresponds to internal heat absorption.

Thermal radiation is simulated using the Rosseland diffusion approximation and in accordance with this, the radiative heat flux q_r is given by

$$q_r = -\frac{4\sigma^*}{3k^*}\frac{\partial T^4}{\partial y} \quad (8)$$

Where σ^* is the Stefan–Boltzman constant and k^* is the Rosseland mean absorption coefficient. If the temperature differences within the mass of blood flow are sufficiently small, then Eq. (8) can be linearized by expanding T^4 into the Taylor's series about T_∞, and neglecting higher-order terms, we get

$$T^4 \cong 4T_\infty^3 T - 3T_\infty^4 \quad (9)$$

We introduce the self-similar transformations (see Chamka et al., [31] Srinivas et al., [17] and Misra and Sinha[32])

$$\eta = \left(\frac{U_w}{vx}\right)^{\frac{1}{2}} y, \quad \psi = (vxU_w)^{\frac{1}{2}} f(\eta),$$

$$\theta(\eta) = \frac{T - T_\infty}{T_w - T_\infty}, \phi(\eta) = \frac{C - C_\infty}{C_w - C_\infty}, \quad (10)$$

Where η is the similarity variable and ψ is the stream function. The velocity components are

$u = \frac{\partial \psi}{\partial y}$, $v = -\frac{\partial \psi}{\partial x}$, which identically satisfies Eq. (1).

Now substituting (9) and (10) into the Eqs. (2) – (4), we get the following set of ordinary differential equations

$$f''' + ff'' - (f')^2 - A\left(f' + \frac{1}{2}\eta f''\right) + Gr\theta\cos\alpha + Gc\phi\cos\alpha - M^2 f'\sin^2\xi - \frac{1}{K_3}f' = 0 \quad (11)$$

$$\frac{(1+R)}{p_r}\theta'' + f\theta' - f'\theta - A\left(\theta + \frac{1}{2}\eta\theta'\right) + \frac{\left(A^* f' + B^*\theta\right)}{p_r} + Ec(f')^2 = 0 \quad (12)$$

$$\frac{1}{Sc}\phi'' + f\phi' - f'\phi - A\left(\phi + \frac{1}{2}\eta\phi'\right) - \gamma\phi = 0 \quad (13)$$

where *A; M; K_3; Gr; Gc; R; Pr; Ec; Sc* and γ are non-dimensional parameters called, respectively, the unsteadiness parameter, Hartmann number, permeability parameter, Grashof number, solutal Grashof number, radiation parameter, Prandtl number, Eckert number, Schmidt number and chemical reaction parameter are given by

$$A = \frac{c}{a}, \quad M = B_0\sqrt{\frac{\sigma}{\rho a}}, K_3 = \frac{ak_2}{\nu}, \quad Gr = \frac{g\beta x(T_w - T_\infty)}{U_w^2},$$

$$Gc = \frac{g\beta^* x(c_w - c_\infty)}{U_w^2}, R = \frac{16\sigma^* T_\infty^3}{3kk^*}, \Pr = \frac{\mu cp}{k},$$

$$Ec = \frac{U_w^2}{c_p(T_w - T_\infty)}, Sc = \frac{\upsilon}{D} \text{ and } \gamma = \frac{\Gamma_0}{a} \quad (14)$$

The corresponding boundary conditions are

$$f = S, \quad f' = 1 + S_f f''(0), \quad \theta = 1 + S_t\theta'(0),$$
$$\phi = 1 + S_c\phi'(0) \text{ at } \eta = 0,$$
$$f' \to 0, \theta \to 0, \phi \to 0, \phi \to 0, \eta \to \infty. \quad (15)$$

In Eq. (15), S < 0 and S > 0 correspond to injection and suction, respectively. The non-dimensional velocity slip S_f

 DOI : 10.18231/2454-9150.2018.1286

thermal slip S_t and solutal slip S_c are defined by

$$S_f = N_0\rho\sqrt{av}\ , \quad S_t = K_0\sqrt{\frac{a}{v}} \ \text{and} \ S_c = P_0\sqrt{\frac{a}{v}}$$

where the prime denotes derivatives with respect to η . It may be noted that when A=0 in Eqs. (11) – (13), the problem will be reduced to the one in the steady state.

Also the quantities of physical interest in this problem are the skin friction coefficient, heat transfer rate and mass transfer which are defined as

$$C_f = \frac{\tau_w}{\frac{\rho U_w^2}{2}}\ , \ Nu_x = \frac{xq_w}{k\left(T_w - T_\infty\right)}\ , \ Sh_x = \frac{m_w x}{\rho D\left(c_w - c_\infty\right)} \qquad (16)$$

Where the wall shear stress, surface heat flux and the mass flux are given by

$$\tau_w = \mu\left(\frac{\partial u}{\partial y}\right)_{y=0}\ , \ q_w = -k\left(\frac{\partial T}{\partial y}\right)_{y=0}\ , \ m_w = -\rho D\left(\frac{\partial c}{\partial y}\right)_{y=0} \qquad (17)$$

Using Eq. (17), quantity (16) can be expressed as

$$C_f = \frac{1}{2}\mathrm{Re}_x^{-\frac{1}{2}} f''(0)\ , \ Nu_x = -\mathrm{Re}_x^{\frac{1}{2}}\theta'(0)\ , \ Sh_x = -\mathrm{Re}_x^{\frac{1}{2}}\phi'(0)\ ,$$

The above skin-friction coefficient, local Nusselt number and Sherwood number show that their variations depend on the variation of the factors $f''(0), -\theta'(0), \text{and} -\phi'(0)$, respectively.

III. ESTIMATES NUMERICAL AND RELATED DISCUSSION

Figures 2– 8 depict the influence of non-dimensional axial velocity for different values of Magnetic parameter, permeability parameter, thermal Grashof number, solutal Grashof number, velocity slip factor, suction parameter, inclination parameter respectively. Figure 2 shows that the velocity lowers as the induced magnetic parameter *M* increases for steady and unsteady flows. This is due to the application of the magnetic field in the Y-direction an electrically conducting fluid gives rise to a flow resistive force called Lorentz force, thereby reducing the magnitude of the velocity.

Figure 3 displays the variations of velocity profile with changes in the permeability parameter. From this figure it can be observed that an increase in the permeability enhances the velocity of the fluid. One can see that, for small permeability (*K* = 0.1), the axial velocity reduces faster than the case when the permeability is higher (*K* = 0.3; 0.5). Further one can note that the same patterns of velocity profiles are observed for steady and unsteady cases.

The variation of the axial velocity for both thermal grashof number (*Gr*) and solutal grashof number (*Gc*) for steady and unsteady flows are shown in figures 4-5. *Gr* signifies the relative effect of the thermal buoyancy force to the viscous hydrodynamic force in the boundary layer regime. An increase in *Gr* or *Gc* induces a rise in the steady and unsteady state velocity profiles. There is a rapid rise in the velocity near the wall and then the velocity descends smoothly towards zero.

Figure 6 presents the velocity profiles for various values of velocity-slip factor. With the increasing values of velocity slip parameter the fluid velocity slightly reduces and then the velocity descends smoothly towards zero. When slip occurs, the fluid flow velocity near the plate is no longer equal to the sheet stretching velocity, i.e., a velocity slip exists. With the rise in S_f such a slip velocity increases. Further it is also observed that the velocity slip is less for unsteady case when compared with steady case.

Figure 7 is aimed to shed light on the effect of suction parameter on the velocity distribution in the boundary layer. It reveals that the velocity profiles decrease with an increase in the suction parameter. This is because the heated fluid is pushed towards the wall where the buoyancy forces can act to retard the fluid due to high influence of viscosity. Same trend is observed for both cases.

From figure 8 we infer that the velocity profiles decrease with an increase in the inclination parameter α. This can be attributed to the fact that the angle of inclination decreases the effect of the buoyancy force due to thermal diffusion by a factor of cosα. Consequently, the driving force to the fluid decreases as a result velocity of the fluid decreases. It is also observed that the inclination is less for unsteady case than the steady case.

Figures 9-14 focus on the temperature distribution for various values of thermal radiation parameter, Prandtl number, unsteadiness parameter, temperature dependent source/sink, Eckert number, thermal slip parameter and inclination. The temperature profiles are presented for various values of thermal radiation parameter in figure 9. It is worthwhile to note that the radiation effect are inversely proportional to the radiation parameter *R* which implies an increase in radiation effect with decrease in *R*. We may observe from figure 9 that the fluid temperature decreases with increasing *R* which helps to conclude that the temperature of the fluid decrease with increasing radiation effects. The fluid particle volume fraction increases near the wall within the boundary layer region and changes its characteristics away from the wall. Same tendency is observe for both steady and unsteady cases.

Figure 10 demonstrates the effect of Prandtl number on the temperature distribution. The numerical results show that an increase in the Prandtl number results in a decrease of the thermal boundary layer thickness and in general lower average temperature within the boundary layer. The reason is that smaller values of *Pr* are equivalent to increasing the thermal conductivity of the fluid, and therefore heat is able to diffuse away from the heated surface more rapidly than higher values of *Pr*. Hence in the case of smaller *Pr*, the thermal boundary layer is thicker and the rate of heat transfer is reduced. Therefore an increase in *Pr* reduces temperature.

Figure 11 represents the temperature profiles for various values of unsteadiness parameter *A*. It is observed from this figure that as the unsteadiness parameter increases, the temperature of the boundary layer also increases.

 DOI : 10.18231/2454-9150.2018.1286

The variations in the temperature profiles for changes in the heat source/sink (*B**) are presented in figure 12. It is observed that the temperature enhances with an increase in heat source.

The effect of Eckert number *Ec*, on temperature is shown in figure 13. Eckert number *Ec*, designates the ratio of the kinetic energy of the flow to the boundary layer enthalpy difference. As *Ec* is enhanced, the velocity as well as the temperature increases, since internal energy is increased. It is also seen from this figure that the temperature is less for unsteady case when compared with steady case near the plate and then the temperature descends smoothly towards zero.

Temperature profiles for the various values of thermal slip parameter S_t are shown in figure 14. It is seen from this figure that the thermal slip parameter increases, less heat is transferred from the stretched wall to the fluid and hence the temperature decreases. It reveals the temperature profiles decreases for both cases.

The computed values of the concentration distribution for various values of solutal slip, Schmidt number and chemical reaction parameter are displayed in figures. 15-17. Figure 15 demonstrates the effect of the solutal slip S_c to the concentration distribution. It indicates that the concentration decreases with a rise in solutal slip.

Figure 16 is a plot of concentration distribution for various values of Schmidt number. The Schmidt number is the ratio between a viscous diffusion rate and a molecular diffusion rate. We notice from this figure that the concentration distribution of the flow field reduces as the Schmidt number increases. This is due to the fact that heavier diffusing species have a greater retarding effect on the concentration distribution of the fluid flow field. Figure 17 shows the influence of the chemical reaction on the concentration profiles in the boundary layer. It reveals that the concentration decreases with an increase in the chemical reaction.

The values $f''(0), -\theta'(0), and -\phi'(0)$ for different values of M^2, K_3, *Gr; Gc; α; R; Pr; A*; B*; Ec; Sc; C* for *A*=0 are shown in Table 1. It can be noted that the skin friction coefficient increased with increasing values of solutal Grashof number and Eckert number, whereas the reverse trend is observed in the case of magnetic parameter, permeability parameter, Grashof number, unsteadiness, thermal radiation, Prandtl number and Schmidt number. Further, from Table 6, it is noticed that the Nusselt number increases with an increase in the Grashof number, permeability parameter, Prandtl number , solutal Grashof number, radiation parameter and the coefficient of space and temperature dependent heat source/sink, where as it decreases with an increase in the magnetic number, inclination, Eckert number, Schmidt number, and chemical reaction. It is observed that the Sherwood number decreases as the suction parameter, radiation parameter, Prandtl number, inclination, Grashof number, permeability parameter increases. It can be seen that the Sherwood number increases with increasing chemical reaction and Schmidt number. On the other hand, the Sherwood number remains same for Eckert number.

The values $f''(0), -\theta'(0), and -\phi'(0)$ for different values of M^2, K_3, *Gr; Gc; α; R; Pr; A*; B*; Ec; Sc; C* for *A*=0.5 are shown in Table 2. It can be noted that the skin friction coefficient increased with increasing values of Grashof number, solutal Grashof number, Prandtl number, permeability parameter and chemical reaction, whereas the reverse trend is observed in the case of magnetic parameter, inclination, unsteadiness, thermal radiation, Prandtl number and Schmidt number. Further, from Table 2, it is noticed that the Nusselt number increases with an increase in the Grashof number, permeability parameter, Prandtl number , solutal Grashof number, radiation parameter and the coefficient of space and temperature dependent heat source/sink, where as it decreases with an increase in the magnetic number, inclination, Eckert number, Schmidt number and chemical reaction. It is observed that the Sherwood number decreases as the suction parameter, radiation parameter, Prandtl number, inclination, Grashof number, permeability parameter increases. It can be seen that the Sherwood number increases with increasing chemical reaction and Schmidt number. On the other hand, the Sherwood number remains same for Eckert number.

The values of $f''(0), -\theta'(0), and -\phi'(0)$ for different values of S_f, S_t and S_c for *A*=0 are shown in Table 3. The skin-friction coefficient decreases with the thermal slip and concentration slip, while it increases with the velocity slip. The Nusselt number decreases with the thermal slip and concentration slip while a slight increment is seen for enhancement of velocity slip. It is seen that the value of Sherwood number remains same with an increase of velocity and thermal slip. However, it decreases with an increase of concentration slip.

The values of $f''(0), -\theta'(0), and -\phi'(0)$ for different values of S_f, S_t and S_c for *A*=0.5 are shown in Table 4. The skin-friction coefficient slightly decreases with the thermal slip and concentration slip, while it increases with the velocity slip. The Nusselt number decreases with the thermal slip and concentration slip while a slight increment is seen for enhancement of velocity slip. It is seen that the value of Sherwood number remains same with an increase of velocity and thermal slip. However, it decreases with an increase of concentration

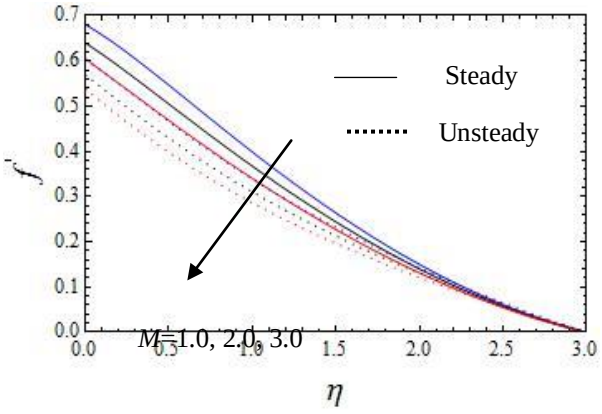

Fig.**2**. Velocity profile for different values of *M*

 DOI : 10.18231/2454-9150.2018.1286

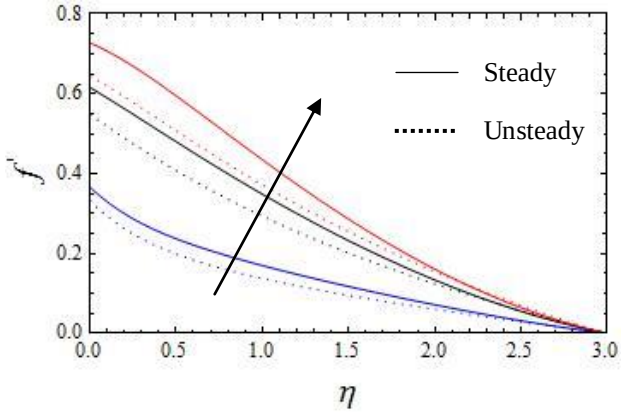

Fig.**3**. Velocity profile for different values of K

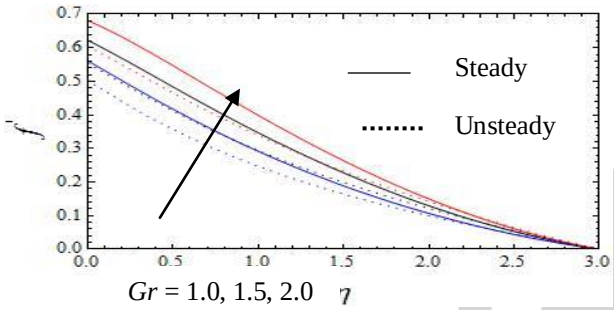

Fig.**4**. Velocity profile for different values of Gr

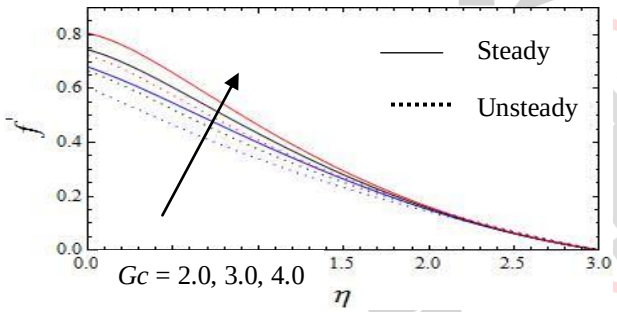

Fig.**5**. Velocity profile for different values of Gc

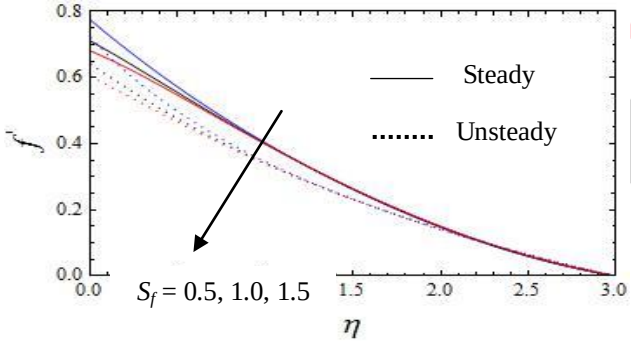

Fig.**6**. Velocity profile for different values of S_f

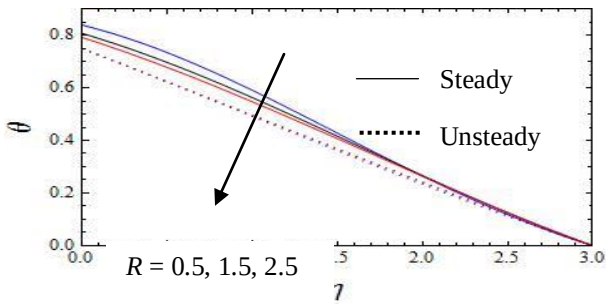

Fig.**8**. Velocity profile for different values of α

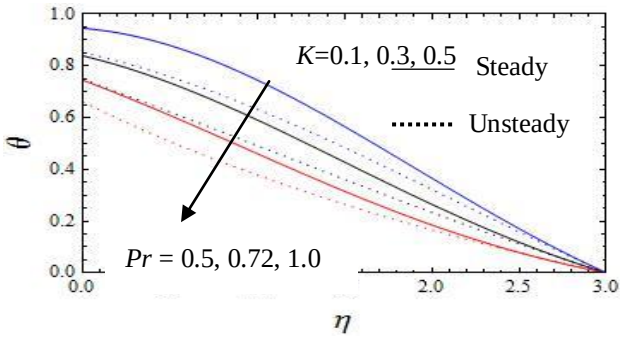

Fig.**9**. Temperature profile for different values of R

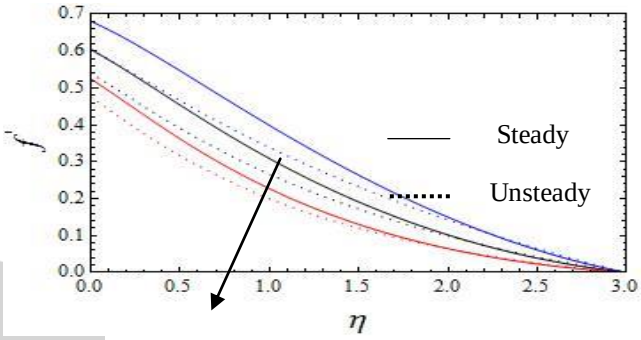

Fig.**10**. Temperature profile for different values of S

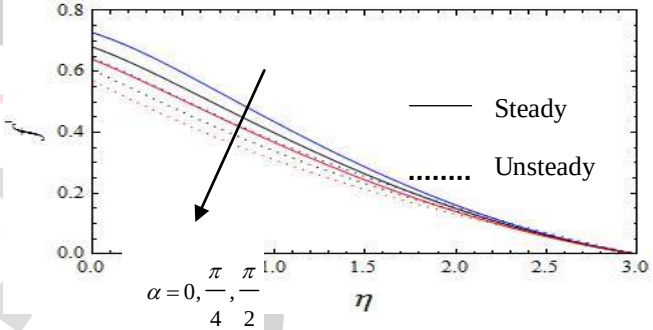

Fig.**10**. Temperature profile for different values of Pr

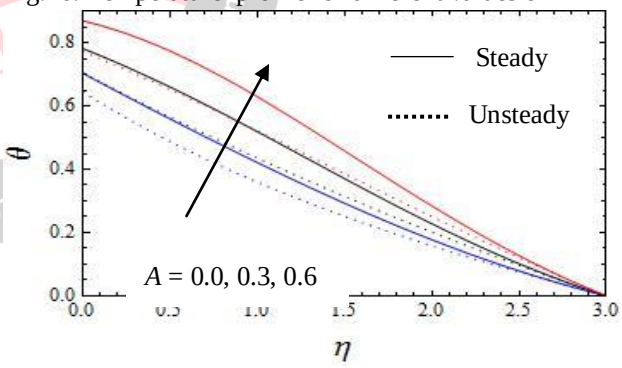

Fig.**11**. Temperature profile for different values of A

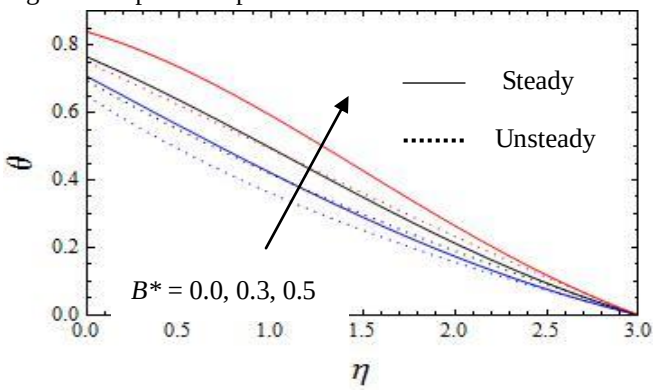

Fig.**12**. Temperature profile for different values of B^*

 DOI : 10.18231/2454-9150.2018.1286

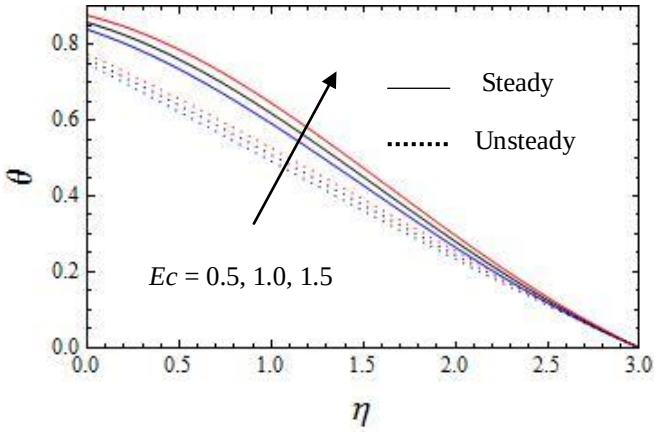

Fig.**13**. Temperature profile for different values of *Ec*

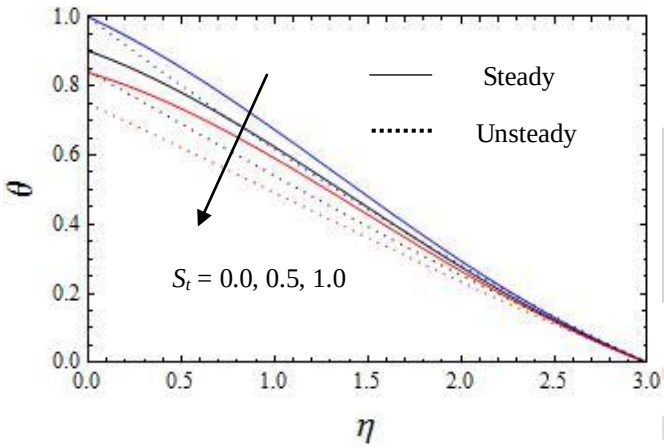

Fig.**14**. Temperature profile for different values of S_t

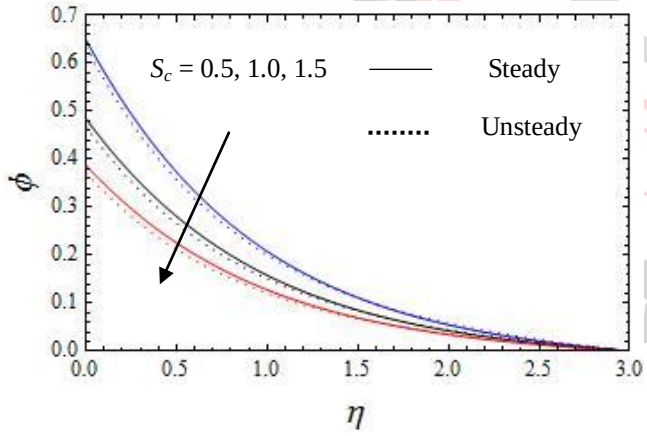

Fig.**15**. Concentration profile for different values of S_c

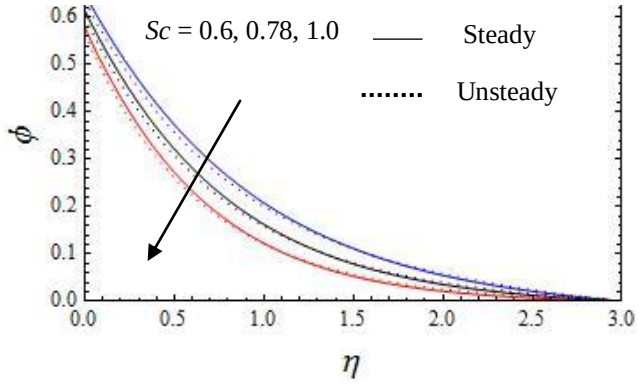

Fig.**16**.Concentration profile for different values of *Sc*

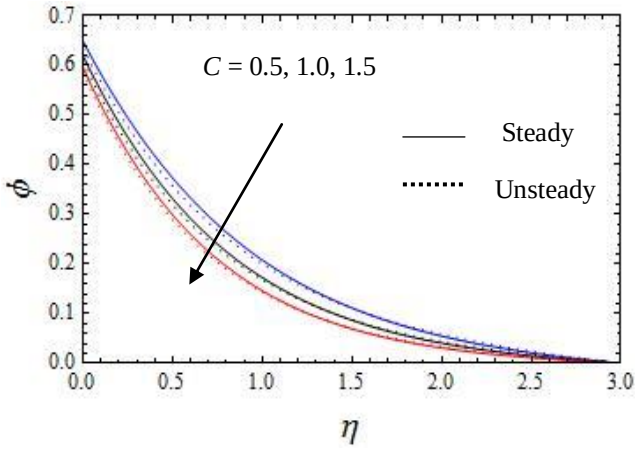

Fig.**17**. Concentration profile for different values of *C*

Table 3. Values of $f''(0), -\theta'(0)\ and\ -\phi'(0)$ for A=0

S_f	S_t	S_c	$f''(0)$	$-\theta'(0)$	$-\phi'(0)$
0.5	0.5	0.5	-0.4284	0.193419	0.711930
1.0	0.5	0.5	-0.274811	0.195771	0.706551
0.5	1.0	0.5	-0.449596	0.157793	0.709203
0.5	0.5	1.0	-0.47589	0.189120	0.522077

Table 4. Values of $f''(0), -\theta'(0)\ and\ -\phi'(0)$ for A=0.5

S_f	S_t	S_c	$f''(0)$	$-\theta'(0)$	$-\phi'(0)$
0.5	0.5	0.5	-0.527545	0.305941	0.743065
1.0	0.5	0.5	-0.338107	0.310468	0.737009
0.5	1.0	0.5	-0.557709	0.244537	0.739663
0.5	0.5	1.0	-0.573978	0.303252	0.539268

IV. CONCLUSION

The steady two-dimensional heat and mass transfer on the MHD flow over an inclined permeable stretching surface with non uniform heat source/sink were numerically investigated. The governing boundary layer equations were reduced into a system of ordinary differential equations and then the equations were solved numerically. The main results of the present investigation are as follows:

- By increasing Ec, the boundary layer as well as the temperature profiles on the stretching sheet are increased.
- By increasing R, the boundary layer of the fluid flow is decreased as well as convective heat transfer rate on the stretching sheet is decreased.
- By increasing Pr, the boundary layer of the fluid flow and the heat transfer rate decreases.
- It can be noted that the skin friction coefficient increased with increasing values of *Gr*, *Gc*, *Pr*, K_3, and γ, whereas the reverse trend is observed in the case of M, ξ, A, R, and *Sc*.

 DOI : 10.18231/2454-9150.2018.1286

M^2	K_3	Gr	Gc	A	R	Pr	A^*	B^*	Ec	Sc	C	$f''(0)$	$-\theta'(0)$	$-\phi'(0)$
1.0	0.4	2.0	2.0	$\frac{\pi}{4}$	0.5	0.72	0.5	0.5	0.5	0.6	0.5	-0.212867	0.161136	0.700642
2.0	0.4	2.0	2.0	$\frac{\pi}{4}$	0.5	0.72	0.5	0.5	0.5	0.6	0.5	-0.239919	0.156875	0.691808
1.0	0.6	2.0	2.0	$\frac{\pi}{4}$	0.5	0.72	0.5	0.5	0.5	0.6	0.5	-0.642560	1.32972	0.304884
1.0	0.4	3.0	2.0	$\frac{\pi}{4}$	0.5	0.72	0.5	0.5	0.5	0.6	0.5	-0.642143	1.17700	0.289564
1.0	0.4	2.0	3.0	$\frac{\pi}{4}$	0.5	0.72	0.5	0.5	0.5	0.6	0.5	-0.170064	0.165366	0.71266
1.0	0.4	2.0	2.0	$\frac{\pi}{2}$	0.5	0.72	0.5	0.5	0.5	0.6	0.5	-0.239919	0.156875	0.691808
1.0	0.4	2.0	2.0	$\frac{\pi}{4}$	1.5	0.72	0.5	0.5	0.5	0.6	0.5	-0.220005	0.192709	0.698302
1.0	0.4	2.0	2.0	$\frac{\pi}{4}$	0.5	1.00	0.5	0.5	0.5	0.6	0.5	-0.239126	0.25508	0.690159
1.0	0.4	2.0	2.0	$\frac{\pi}{4}$	0.5	0.72	1.0	0.5	0.5	0.6	0.5	-0.618869	1.35066	0.397211
1.0	0.4	2.0	2.0	$\frac{\pi}{4}$	0.5	0.72	0.5	1.5	0.5	0.6	0.5	-0.454887	0.893873	0.568339
1.0	0.4	2.0	2.0	$\frac{\pi}{4}$	0.5	0.72	0.5	0.5	1.0	0.6	0.5	-0.207615	0.142452	0.702685
1.0	0.4	2.0	2.0	$\frac{\pi}{4}$	0.5	0.72	0.5	0.5	0.5	0.78	0.5	-0.222889	0.159087	0.770859
1.0	0.4	1.0	2.0	$\frac{\pi}{4}$	0.5	0.72	0.5	0.5	0.5	0.6	1.0	-0.220975	0.159539	0.75916

Table 1. Values of $f''(0), -\theta'(0)$ *and* $-\phi'(0)$ for A= 0

M^2	K_3	Gr	Gc	A	R	Pr	A^*	B^*	Ec	Sc	C	$f''(0)$	$-\theta'(0)$	$-\phi'(0)$
1.0	0.4	2.0	2.0	$\frac{\pi}{4}$	0.5	0.72	0.5	0.5	0.5	0.6	0.5	-0.264000	0.251033	0.729856
2.0	0.4	2.0	2.0	$\frac{\pi}{4}$	0.5	0.72	0.5	0.5	0.5	0.6	0.5	-0.287270	0.249833	0.723126
1.0	0.6	2.0	2.0	$\frac{\pi}{4}$	0.5	0.72	0.5	0.5	0.5	0.6	0.5	-0.216872	0.253112	0.743175
1.0	0.4	3.0	2.0	$\frac{\pi}{4}$	0.5	0.72	0.5	0.5	0.5	0.6	0.5	-0.199729	0.253959	0.748295
1.0	0.4	2.0	3.0	$\frac{\pi}{4}$	0.5	0.72	0.5	0.5	0.5	0.6	0.5	-0.222787	0.252104	0.740304
1.0	0.4	2.0	2.0	$\frac{\pi}{2}$	0.5	0.72	0.5	0.5	0.5	0.6	0.5	-0.287270	0.249833	0.723126
1.0	0.4	2.0	2.0	$\frac{\pi}{4}$	1.5	0.72	0.5	0.5	0.5	0.6	0.5	-0.263538	0.250253	0.730083
1.0	0.4	2.0	2.0	$\frac{\pi}{4}$	0.5	1.00	0.5	0.5	0.5	0.6	0.5	-0.286566	0.338578	0.722120
1.0	0.4	2.0	2.0	$\frac{\pi}{4}$	0.5	0.72	1.0	0.5	0.5	0.6	0.5	-0.232326	0.125914	0.740281
1.0	0.4	2.0	2.0	$\frac{\pi}{4}$	0.5	0.72	0.5	1.5	0.5	0.6	0.5	-0.505811	1.008930	0.616328
1.0	0.4	2.0	2.0	$\frac{\pi}{4}$	0.5	0.72	0.5	0.5	1.0	0.6	0.5	-0.260656	0.238196	0.730992
1.0	0.4	2.0	2.0	$\frac{\pi}{4}$	0.5	0.72	0.5	0.5	0.5	0.78	0.5	-0.273555	0.250335	0.800037
1.0	0.4	1.0	2.0	$\frac{\pi}{4}$	0.5	0.72	0.5	0.5	0.5	0.6	1.0	-0.220975	0.159539	0.759160

Table 2. Values of $f''(0), -\theta'(0)$ *and* $-\phi'(0)$ for A= 0.5

REFERENCES

[1] L. J. Crane, "Flow past a stretching plate," ZAMP, vol. 21, no. 4 pp.645–647, Jul. 1970.

[2] B. Mohanty, S.R. Mishra, and H.B. Pattanayak, "Numerical investigation on heat and mass transfer effect of micropolar fluid over a stretching sheet through porous media," Alexandria Engineering Journal, Vol. 54, No. 2, pp. 223–232, Jun. 2015.

[3] A. Mastroberardino, "Accurate solutions for viscoelastic boundary layer flow and heat transfer over stretching sheet," Applied Mathematics and Mechanics, vol. 35, No. 2, pp. 133–142, 2014.

[4] R. Byron Bird, Warren E Stewart, and N. Edwin Lightfoot, "Transport phenomena," John Wiley and sons, New York, 1992.

[5] EL. CusslerV, "Diffusion mass transfer in fluid systems," Cambridge University Press, London, UK. 1988.

[6] N.J.Themelis, "Transport and chemical rate phenomena," Taylor & Francis Group, (1995).

[7] C. Midya, "Exact solutions of chemically reactive solute distribution in MHD boundary layer flow over a shrinking surface," Chinese Physics Letters vol.29, No. 2, (2012) 014701.

[8] T. Hayata, M. Imtiaza, A. Alsaedib, and R. Mansoora, "MHD flow of nanofluids over an exponentially stretching sheet in a porous medium with convective boundary conditions," Chin. Phys. B Vol. 23, No. 5, (2014) 054701.

 DOI : 10.18231/2454-9150.2018.1286

[9] P. Bala Anki Reddy, S. Suneetha and N. Bhaskar Reddy, "Numerical study of MHD boundary layer slip flow of a Maxwell nanofluid over an exponentially stretching surface with convective boundary condition," Propulsion and Power Research, Vol. 6, No. 4, pp. 225-232, 2017.

[10] Yan Zhang, Min Zhang, and Shujuan Qi, "Heat and mass transfer in a thin liquid film over an unsteady stretching surface in the presence of thermo solutal capillarity and variable magnetic field," Mathematical Problems in Engineering, Vol. 2016 (2016), Article ID 8521580, 12 pages

[11] Manjula Jonnadula, Padma Polarapu, M. Gnaneswara Reddy and M. Venakateswarlu, "Influence of thermal radiation and chemical reaction on MHD flow, heat and mass transfer over a stretching surface," Procedia Engineering, Vol. 127, pp. 1315-1322, 2015

[12] P. V. S. Narayana and D. H. Babu, "Numerical study of MHD heat and mass transfer of a Jeffrey fluid over a stretching sheet with chemical reaction and thermal radiation," Journal of the Taiwan Institute of Chemical Engineers, Vol. 59, pp. 18–25, 2016.

[13] Manoj Kumar Nayak, Gauranga Charan Dash,and Lambodar Prased Singh, "Heat and mass transfer effects on MHD viscoelastic fluid over a stretching sheet through porous medium in presence of chemical reaction," Propulsion and Power Research, Vol. 5, No. 1, pp. 70–80, Mar. 2016.

[14] S. Mukhopadhyay, "Effect of thermal radiation on unsteady mixed convection flow and heat transfer over a porous stretching surface in porous medium," Int. J. Heat Mass Transf, Vol. 52, No. 13-14, pp. 3261–3265, Jun. 2009

[15] P. Bala Anki Reddy, N. Bhaskar Reddy and S. Suneetha, "Radiation effects on MHD flow past an exponentially accelerated isothermal vertical plate with uniform mass diffusion in the presence of heat source," Journal of Applied Fluid Mechanics, Vol. 5, No. 3, pp. 119-126, 2012.

[16] A. J. Chamkha , A. M. Aly and M. A. Mansour, "Similarity solution for unsteady heat and mass transfer from a stretching surface embedded in a porous medium with suction/injection and chemical reaction effects," Journal Chemical Engineering Communications, Vol. 197, No. 6, pp. 846-858, 2010.

[17] S. Srinivas, P. B. A. Reddy, and B. S. R. V. Prasad, "Effects of chemical reaction and thermal radiation on mhd flow over an inclined permeable stretching surface with non-uniform heat source/sink: an application to the dynamics of blood flow," j. mech. med. biol. Vol. 14, No. 5, 24 pages, 1450067 (2014)

[18] S. Jena, G.C. Dash, and S.R. Mishra, "Chemical reaction effect on MHD viscoelastic fluid flow over a vertical stretching sheet with heat source/sink," Ain Shams Engineering Journal, Vol. 9, No. 4, pp. 1205-1213, 2018.

[19] B. Gebhart, "Effects of viscous dissipation in natural convection," J.Fluid Mechanics, Vol. 14, No. 2, pp. 225-232, 1962.

[20] H.C. Brinkman, "Heat effects in capillary flow I," Appl. Sci. Res A2, pp. 120-124, 1951.

[21] G. Chand and R.N. Jat, "Viscous dissipation and radiation effects on MHD flow and heat transfer over an unsteady stretching surface in a porous medium," Therm. Energy Power Engg, Vol. 3, No. 3, pp. 266-272, 2014.

[22] S. Suneetha, N. Bhaskar Reddy and V. Ramachandra Prasad, "Radiation and mass transfer effects on MHD free convective dissipative fluid in the presence of heat source/sink," Journal of Applied Fluid Mechanics, Vol. 4, No. 1, pp. 107-113, 2011.

[23] P. Bala Anki Reddy and S. Suneetha, "Impact of Cattaneo-Christov Heat Flux In the Casson Fluid Flow Over a Stretching Surface With Aligned Magnentic Field and Homogeneous Heterogeneous Chemical Reaction" Frontiers in Heat and Mass Transfer (FHMT), Vol. 10, No. 7, 2018, DOI: 10.5098/hmt.10.7

[24] Mitiku Daba, and Ponnaian Devaraj, "Unsteady hydromagnetic chemically reacting mixed convection flow over a permeable stretching surface with slip and thermal radiation," Journal of the Nigerian Mathematical Society, Vol. 35, No. 1, pp. 245–256, 2016.

[25] K. Das, "Slip flow and convective heat transfer of nanofluids over a permeable stretching surface," Comput. Fluids, vol. 64, pp. 34–42, 2012

[26] Swati Mukhopadhyay, "Slip effects on MHD boundary layer flow over an exponentially stretching sheet with suction/blowing and thermal radiation," Ain Shams Engineering J, vol. 4, No.3, pp. 485-491, 2013.

[27] P. Bala Anki Reddy and S. Suneetha, "Effects Of homogeneous-heterogeneous chemical reaction and slip velocity on Mhd stagnation flow of a micropolar fluid over a permeable stretching/shrinking surface embedded in a porous medium," Frontiers in Heat and Mass Transfer (FHMT), Vol. 8, No. 24, 2017, DOI: 10.5098/hmt.8.24

[28] G. Charan Kumar, K. Jayarami Reddy, K. Ramakrishna and M. Narendradh Reddy "Non-Uniform Heat Source/Sink and Joule Heating Effects on Chemically Radiative MHD Mixed Convective Flow of Micropolar Fluid Over a Stretching Sheet in Porous Medium,". Defect & Diffusion Forum, vol. 388, pp. 281-302, 2018.

[29] S. Mohammed. Ibrahim, prathi, Vijaya Kumar, and CSK. Raju "Possessions of viscous dissipation on radiative MHD heat and mass transfer flow of a micropolar fluid over a porous stretching sheet with chemical reaction," Trans. Phenom. Nano Micro Scales, vol. 6 no. 1, pp. 60-71, winter and spring 2018. DOI: 10.7508/tpnms.2018.01.006

[30] K. Jayarami Reddy, N.P. Madhusudhana Reddy, K. Ramakrishna and D. Abhishek, "Effect of non-uniform heat source/sink on MHD boundary layer flow and melting heat transfer of Williamson nanofluid in porous medium," Multidiscipline Modeling in Materials and Structures, https://doi.org/10.1108/MMMS-01-2018-0011

[31] A. J. Chamka, A. M. Aly, and M. A. Mansour, "Similarity solution for unsteady Heat and mass transfer from a stretching surface embedded in a porous medium with suction/injection and chemical reaction effects," Chem Eng Comm, Vol. 197, No.6, pp. 846–858, 2010.

[32] J. C. Misra, and A. Sinha, "Effect of thermal radiation on MHD flow of blood and heat transfer in a permeable capillary in stretching motion," Heat Mass Transfer, Vol. 49, No. 5, pp. 617–628, 2013.

 DOI : 10.18231/2454-9150.2018.1286